

Volume Compensation Method for Routing Irrigation Canal Demand Changes

E. Bautista, A.M.ASCE,¹ and A. J. Clemmens, M.ASCE²

Abstract: This paper examines the problem of routing known water demands through gate-controlled, open-channel irrigation delivery systems. Volume-compensation principles were used to route multiple demands in multiple-pool canal systems. The volume-compensation method schedules each demand change individually under the assumption of a series of steady states and superimposes the individual results. Volume-compensation routing schedules were computed for two of the test cases proposed by the ASCE Task Committee on Canal Automation. Alternative routing schedules were computed with the gate-stroking method, which is an inverse solution of the unsteady-flow equations. Both solutions were tested through unsteady-flow simulation. While not as effective as gate-stroking solutions, volume-compensation solutions performed satisfactorily under ideal flow control conditions. When subjected to realistic operational constraints, specifically constraints on the flow regulation interval, and also to incorrect canal hydraulic roughness information, both methods performed similarly.

DOI: 10.1061/(ASCE)0733-9437(2005)131:6(494)

CE Database subject headings: Open channel flow; Flow control; Computer aided scheduling; Routing; Delay time; Volume change; Irrigation districts; Canals; Water demand.

Introduction

A key irrigation delivery system control problem is routing known (or predicted) demand changes. Because inflow perturbations can take hours or even days to travel to downstream delivery points, check-structure operations often need to be scheduled in anticipation of the known demand changes. The scheduled operations must not disrupt ongoing deliveries, must deliver the anticipated demand changes accurately and on time, and must not require unreasonable control actions. This problem can be described as the feedforward control (anticipatory, open-loop) problem of open-channel flow. The paper summarizes recent research conducted in the area of feedforward control. A simple control approach is described, based on the principle of volume compensation. This research is part of an effort to develop a comprehensive automated control system for open-channel irrigation delivery systems.

Gate-Stroking Solutions to Canal Routing Problem

Gate stroking was proposed more than 30 years ago as a method for solving the canal feedforward control problem (Wylie 1969). The method consists of an inverse solution to the unsteady open-channel flow equations: given a desired schedule of offtake discharges, it determines check-structure discharge variations needed to produce such deliveries. The solution is computed by setting the water level upstream from check structures equal to the desired forebay setpoint depth or by imposing a desired level variation as a function of time, for known initial conditions. Because of unsteady-flow effects, initial conditions generally are not known and steady conditions have to be assumed. The method has not been adopted for field applications, partly due to computational difficulties. The inverse problem is poorly posed mathematically (Cunge et al. 1980), meaning that small changes in the input data can cause substantial changes in the shape of the computed inflow hydrographs. Also, gate stroking sometimes produces solutions requiring extreme and unrealistic inflow variations (such as flow reversals) or no solution at all.

While not practical, the gate-stroking concept has proved useful for studying the characteristics of the feedforward control problem. Just as small changes in the input data can cause substantial changes in the form of the solution, comparable water-level control can be achieved with seemingly different gate-stroking solutions. This was demonstrated by comparing the effectiveness of gate-stroking solutions computed with a method-of-characteristics algorithm (Falvey and Luning 1979) and with a finite-difference algorithm (Bautista et al. 1997). Solutions obtained with the latter method were numerically damped in comparison with the former (the hydrographs exhibited smaller flow peaks), but the resulting water-level control was similar.

¹Research Hydraulic Engineer, USDA-ARS U.S. Water Conservation Laboratory, 4331 E. Broadway Rd., Phoenix, AZ 85040. E-mail: ebautista@uswcl.ars.ag.gov

²Research Hydraulic Engineer and Laboratory Director, USDA-ARS U.S. Water Conservation Laboratory, 4331 E. Broadway Rd., Phoenix, AZ 85040. E-mail: bclemmens@uswcl.ars.ag.gov

Note. Discussion open until May 1, 2006. Separate discussions must be submitted for individual papers. To extend the closing date by one month, a written request must be filed with the ASCE Managing Editor. The manuscript for this paper was submitted for review and possible publication on November 19, 2003; approved on January 4, 2005. This paper is part of the *Journal of Irrigation and Drainage Engineering*, Vol. 131, No. 6, December 1, 2005. ©ASCE, ISSN 0733-9437/2005/6-494-503/\$25.00.

Table 1. Canal and Scheduled Demand Data for Test Case 1-2

Pool number	Length (km)	Target depth (m)	Initial offtake flow (m ³ /s)	Initial pool inflow (m ³ /s)	Offtake flow change (m ³ /s)	Final pool inflow (m ³ /s)
1	0.1	0.9	0.2	2.0	0.0	2.0
2	1.2	0.9	0.2	1.8	-0.2	1.8
3	0.4	0.8	0.2	1.6	0.2	1.8
4	0.8	0.9	0.2	1.4	-0.2	1.4
5	2.0	0.9	0.2	1.2	-0.2	1.4
6	1.7	0.8	0.2	1.0	0.1	1.4
7	1.6	0.8	0.2	0.8	0.0	1.1
8	1.7	0.8	0.6	0.6	0.3	0.9

In a subsequent study, gate-stroking solutions were modified by allowing flow changes to occur only at a specified regulation time interval (an interval much larger than the time step used in the calculations) and by allowing only flow-rate changes greater than a tolerance value (Bautista and Clemmens 1999b). The modified hydrographs were forced to deliver the same total volume of water during the transient as the original solutions. Again, control performance did not differ greatly between solutions when measured on the basis of the average absolute deviation over a test period (although the modified solution did result in larger but short-lived water-level deviations).

The behavior of gate-stroking solutions to the single-pool, single-demand problem has been examined in detail (Bautista et al. 2003). That study was restricted to prismatic canals of uniform slope subject to a single step change in demand at the downstream boundary, but a wide range of geometrical and flow conditions were tested. Nondimensional forms of the governing equations (Strelkoff and Clemmens 1998) were used to reduce the number of independent variables considered. The analysis aimed to identify conditions under which gate-stroking solutions become impractical (requiring flow changes much larger than the prescribed demand change) or even infeasible.

Results showed that the magnitude of peak inflows required by gate-stroking solutions increases nonlinearly with the ratio of pool volume change over travel time (calculated under the initial flow conditions). For a single pool subject to a single demand change, a routing strategy based simply on volume compensation, that is, on delivering the canal storage change needed for the new steady condition over a predetermined time, performed nearly as well as gate stroking. Hence, and as noted by Deltour (1992) and Parrish (1997), pool-volume adjustments are key to the canal control problem. The volume-compensating routing strategy is discussed in a later section.

Additivity of Gate-Stroking Solutions

Most routing problems of practical interest deal with multiple pools subject to multiple demand changes. The infinite number of flow configurations precludes an exhaustive analysis of their feedforward control characteristics, as was done for single-pool, single-change cases. However, general findings from the simple cases can be extrapolated to complex situations if the latter can be treated as a series of individual, linearly additive routing problems. The linearity of gate-stroking solutions has been examined for a specific canal system (Bautista et al. 2002). We expand on those results here.

The analysis is based on the two test canals suggested by the ASCE Task Committee on Canal Control Algorithms. See Clemmens et al. (1998), which provides detailed physical characteristics of those canals. Canal 1, which is 9.5 km (5.9 mi) long, is steep and has little storage volume, while the 28 km (17.4 mi) long Canal 2 is relatively flat and has significant storage. Both canals consist of eight pools, each controlled by an undershot gate and supplying a single turnout. For Canal 1, the scenario studied consists of flow changes at six of the turnouts 2 h after the beginning of the test. Demand and pool flow rates, demand changes, and final pool discharges are given in Table 1. This test case is identified as TC1-2, and the scenario studied for Canal 2, which also consists of six simultaneous flow changes after 2 h (Table 2), is identified as TC2-2.

Two solutions were developed for each test case. The first was a conventional gate-stroking solution, in which all demand changes are processed simultaneously. Required inputs and program outputs were described earlier. The solution assumed initial steady conditions. Simultaneous solutions for TC1-2 and TC2-2

Table 2. Canal and Scheduled Demand Data for Test Case 2-2

Pool number	Length (km)	Target depth (m)	Initial offtake flow (m ³ /s)	Initial pool inflow (m ³ /s)	Offtake flow change (m ³ /s)	Final pool inflow (m ³ /s)
1	7.0	2.1	0.2	2.7	1.5	13.7
2	3.0	2.1	0.3	2.5	1.5	12.0
3	3.0	2.1	0.2	2.2	2.5	10.2
4	4.0	1.9	0.3	2.0	0.0	7.5
5	4.0	1.9	0.2	1.7	0.0	7.2
6	3.0	1.7	0.3	1.5	0.5	7.0
7	2.0	1.7	0.2	1.2	1.0	6.2
8	2.0	1.7	0.3	1.0	4.0	5.0

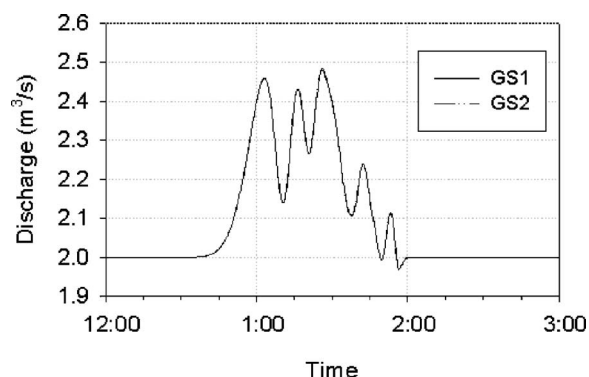


Fig. 1. Simultaneous and superposition gate-stroking solutions computed for headgate in Test Case 1-2

have been previously presented and shown to produce satisfactory water level control (Bautista and Clemmens 1999b).

The second solution was obtained by applying superposition: a gate-stroking solution was computed for each demand change individually, each subject to its own initial conditions, and then a global solution was obtained by adding the individual problem outputs. Global solutions for each check structure were obtained by converting the inflow hydrographs calculated for each individual demand problem into flow increment schedules and then adding the flow increment schedules, time step by time step, to the check structure's initial flow $Q_k(0)$.

Initial conditions for solving individual routing problems are difficult to determine precisely because transient conditions created by a first demand change may have not disappeared by the time a second demand change is being routed. Approximate initial conditions can be determined, however, if one assumes that each individual demand change generates a new steady state. The only difficulty is determining the sequence of hypothetical steady states applicable to each individual problem. For the scenarios tested here, determining that sequence is straightforward: the first demand change to affect canal flows and levels is the one with the longest travel time. Therefore, the most downstream demand change was processed first, and that change was used to compute the initial canal flows and levels for the next upstream demand change. This process was continued until routing the most upstream demand change, which has the shortest travel time.

Fig. 1 depicts the hydrographs computed at the head of the canal for Test TC1-2. The simultaneous (GS1) and superposition (GS2) solutions are indistinguishable at the scale of the graph. Similarly, hydrographs computed for other check structures but not shown here were nearly identical. Results, therefore, support the linearity assumption. Two factors need to be considered when interpreting these findings. First, the canal has a relatively high Froude number under the proposed flow conditions (about 0.8 for all pools). Because transient effects tend to dissipate rapidly under such conditions, near-steady flow conditions may prevail by the time successive demand changes take place. Second, the test consists of relatively mild flow changes with no net inflow change at the head of the canal. As a result, initial conditions associated with each individual demand change are not very different from each other. Therefore, the test represents conditions under which the linearity assumption would be most likely to hold.

In contrast, Test TC2-2 represents conditions under which strong flow nonlinearities can be expected. This canal is entirely affected by backwater, with low flow velocities and Froude numbers (about 0.16) in all pools, and therefore transient conditions

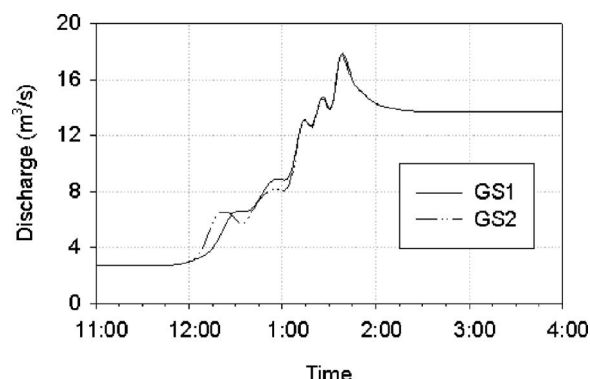


Fig. 2. Simultaneous and superposition gate-stroking solutions computed for headgate in Test Case 2-2

can be expected to persist for a long time. In addition, the test involves larger flow changes than TC1-2, and the initial conditions used to process each individual problem are substantially different from each other. Despite these differences, the simultaneous (GS1) and superposition (GS2) solutions produced headgate hydrographs that were not very different from each other (Fig. 2). Hydrographs for other check structures were also similar.

Two things should be noted. First, differences between the schedules are most pronounced during the initial part of the transient as a result of the demand change in Pool 8, which is larger than the initial canal inflow and thus the source of strong nonlinearities ($4.0 \text{ m}^3/\text{s}$ [141.3 cfs] versus $2.7 \text{ m}^3/\text{s}$ [95.3 cfs]; see Table 2). Second, despite differences in the shape of the hydrographs, the time integral of both curves can be shown to be the same. Hence, if the sequence of steady states (and thus initial conditions associated with each individual routing problem) is properly determined, then the volume delivered by the superposition solution matches the volume delivered by the simultaneous solution.

Additional tests have been conducted with these canals under other combinations of initial conditions and offtake demand schedules. Results not documented here have further shown that gate-stroking solutions to complex scheduling problems can be developed as the sum of solutions to single-demand scheduling problems. Superposition works better when demand changes are small relative to total canal inflow, but it still yields reasonable results when demand changes are relatively large. This suggests we can also superimpose single-demand routing schedules developed by simple procedures, as long as those schedules provide reasonable performance. Key to applying superposition is to properly account for the initial conditions of each individual demand change, and therefore needed pool volume changes.

Simplified Routing by Volume Compensation

The volume-compensation routing strategy is, in essence, a refinement of current heuristic approaches employed by canal operators who base their decisions on travel time alone, without accounting for volume changes. It is also the foundation for the dynamic regulation method, which is used to control the Canal de Provence (Deltour 1992). The concept is discussed first for the single-pool, single-demand problem (Fig. 3). Given a downstream demand change Δq_d , pool volume must be adjusted by an amount ΔV , the difference in pool volume between the assumed initial

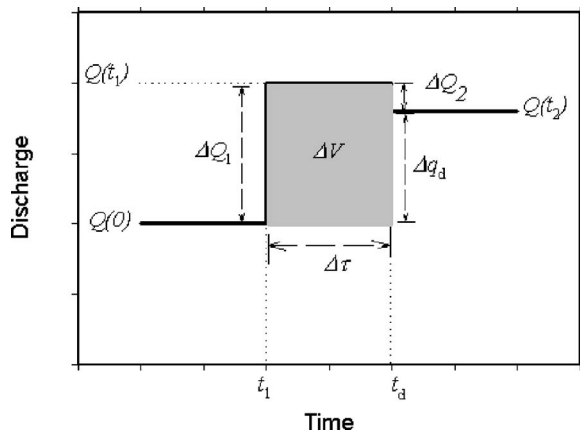


Fig. 3. Volume-compensation concept

and final steady states (the shaded area in Fig. 3). If the demand change is requested at a time t_d , an initial pool inflow rate change ΔQ_1 is made at a time t_1 , where t_1 is the difference between the demand time t_d and the perturbation wave travel time (i.e., the pool delay) $\Delta\tau$. The magnitude of ΔQ_1 is given by the ratio ΔV and $\Delta\tau$; hence, ΔQ_1 supplies the needed volume change. A second pool inflow change ΔQ_2 is needed at t_d to balance the final pool inflow and outflow. The volume-compensation schedule can then be written as

$$\Delta Q_1 = \frac{\Delta V}{\Delta\tau}; \quad t_1 = t_d - \Delta\tau \quad (1)$$

$$\Delta Q_2 = \Delta q_d - \Delta Q_1; \quad t_2 = t_d$$

In the following paragraphs, Subscripts 1 and 2 are used to denote, respectively, the first and second flow rate change required by the volume compensation method. The following sections discuss ΔV and $\Delta\tau$ calculations and the extension of the procedure to multiple-pool, multiple-change problems.

Pool Volume Relationships

The volume of water stored in a pool, V , is a function of canal geometry, hydraulic roughness (n if using the Manning formula), and boundary conditions (inflow rate Q_{in} , lateral inflows and outflows q , downstream outflow rate Q_{out} , and the forebay water-level setpoints y_{stp}). Standard steady-flow calculations can be used to determine V . A scheduling problem involving multiple demand changes can require hundreds of volume calculations. Therefore, for repeated volume calculations, a simpler and more robust approach is to develop tables of V as a function of the dependent variables, covering the range of flow conditions to be encountered, and to interpolate from those tables (Bautista and Clemmens 1999a). Evidently such tabulation can be complex, depending on how V varies as a function of the independent variables and the number of lateral flow structures that need to be considered.

An understanding of pool volume relationships is needed to develop concise yet accurate tables. An example is presented in Fig. 4, for a simple pool without lateral inflows and outflows (i.e., $Q_{in} = Q_{out}$). Each curve represents the Q_{in} - V relationship for a specific combination of Manning n and y_{stp} . Backwater affects the entire length of this pool with the selected y_{stp} values. The tabulation for such a case is simple, not only because it depends on three variables only, but because V changes very gradually as a

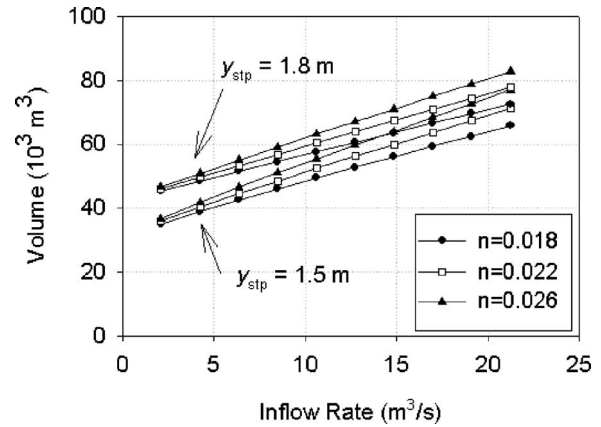


Fig. 4. Storage volume as function of inflow rate, Manning n , and downstream water level setpoint for example canal pool

function of those variables. Interpolated volume estimates can be expected to be reasonably accurate, even if the volumes are calculated at relatively coarse increments of the independent variables. Pools with sharp slope changes and supercritical flow sections exhibit abrupt volume variations and would require a more detailed analysis than shown in the figure.

Figs. 5 and 6 illustrate the effect of offtake discharge on discharge-volume relationships. Both examples are based on an identical 2.6 km pool except for the location of a 17 m³/s capacity offtake. In Fig. 5, the offtake is located 100 m upstream from the pool's end, and in Fig. 6, 1.5 km (the latter case represents the actual pool). Both graphs were developed for the same Manning n and y_{stp} combination. An offtake located right next to the boundary yields a Q_{in} - V relationship identical to one developed by ignoring the offtake discharge q (i.e., by assuming that $Q_{in} = Q_{out}$ for any value of q). That case is represented by the $q=0$ curve in either Fig. 5 or Fig. 6.

Moving the offtake upstream causes the Q_{in} - V relationship to shift downward. The magnitude of the shift depends on both location and q . Hence, the shift is slight for any q when the offtake is located 100 m upstream, but is much larger when it is located 1.5 km upstream. In Fig. 5, if we ignore the offtake location, that is, $Q_{in} = Q_{out}$, the volume prediction error will be at most 3% when both the pool and offtake are discharging at capacity (39.6 m³/s [1,400 cfs] and 17.0 m³/s [600 cfs], respectively). The volume change prediction error will be much smaller, especially when dealing with small demand changes. Therefore, the Q_{in} - V tables for this example can be simplified by assuming $Q_{in} = Q_{out}$.

In the example of Fig. 6, ignoring q will result in a volume prediction error in excess of 14% when the system is at capacity. More important, the volume change prediction error will be nearly as large if, under those initial conditions, the offtake shuts down (note however that the volume change prediction error will be much smaller if the inflow decreases as a result of demand changes downstream from the pool). Volume tables for this pool need to include the offtake as an independent variable.

The following general guidelines are offered when developing pool volume tables. In pools entirely affected by backwater, V varies gently as a function of discharge. Volumes for such pools can be tabulated at relatively coarse increments of the independent variables. The Q_{in} - V relationships for pools with offtakes located close to the downstream boundary, which is a typical pool configuration, are very similar to those obtained when $Q_{in} = Q_{out}$.

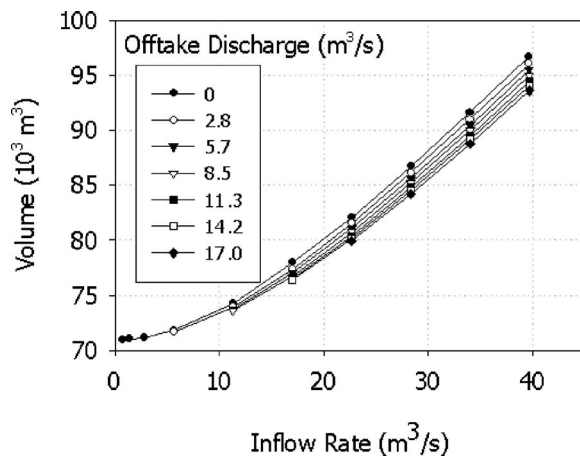


Fig. 5. Storage volume as function of inflow rate and offtake discharge for example canal pool with fixed Manning n and downstream water level setpoint with offtake located near pool's downstream boundary

No special tabulation is needed for that type of pool. Similarly, lateral inflows located near the upstream boundary have little influence on the water surface profile and can be added to the upstream inflow. In cases where an offtake (or intake) is located midway through a pool, discharge-volume relationships generally need to be developed with the structure as an additional independent variable. However, the structure's effect can be ignored if its capacity is small relative to the pool inflow and the pool is entirely under backwater. In all cases, the accuracy of tables has to be verified by comparing simulated and interpolated values.

The volume tables can be further simplified by fitting the data to an empirical equation. For cases where, without lateral flows, a modified power function has been found to fit the data well

$$V = a \cdot Q_{in}^b + c \quad (2)$$

where a , b , and c are fitted parameters, with one set computed for each Manning n and y_{stp} combination. Note that the volume does not go to zero with zero flow since water remains ponded at the setpoint elevation. For cases in which one or two lateral flows need to be tabulated, the following equation is recommended:

$$V = a \cdot Q_{in}^b + c + \sum_{j=1}^J d_j \cdot q_j \cdot Q_{in} \quad (3)$$

In Eq. (3), J is the total number of lateral flows, d is a fitted parameter, and q has a positive or negative sign, depending on whether it is an inflow or outflow, respectively. In cases with more than one lateral flow structure, two or more of those structures can be combined. Our experience analyzing volume relationships for a wide variety of pools so far suggests that many pools can be described with reasonable accuracy without accounting for offtakes or by just including one combined offtake in the tabulation. Therefore, no efforts have been made to use Eq. (3) with more than two large lateral flows.

Delay Calculations

A well-timed feedforward change will minimize forebay water-level fluctuations. Determining travel time is difficult, however, because perturbation waves attenuate as they travel downstream, resulting in a gradual arrival of flow changes.

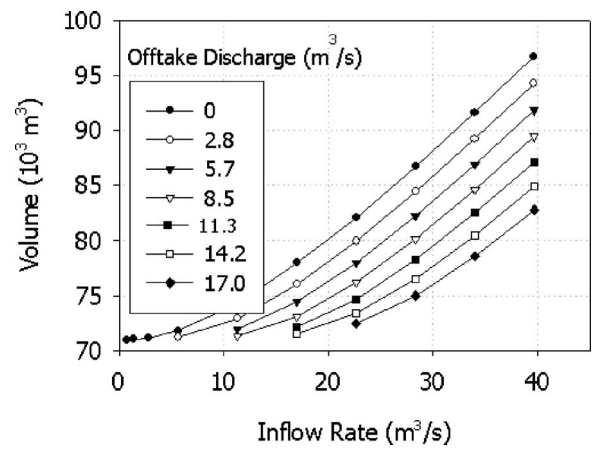


Fig. 6. Storage volume as function of inflow rate and discharge for same example as in Fig. 5 but with offtake located midway through pool

Previous studies have used dynamic wave and kinematic wave theory to predict delays in natural streams, regulated open-channel systems, and sewers (Henderson 1966; Corrigan et al. 1982; Papageorgiou and Messmer 1985). A delay based on dynamic wave theory, $\Delta\tau_{DW}$, is given by

$$\Delta\tau_{DW} = \frac{L}{v_{DW0}} = \frac{L}{v_0 + c_0} \quad (4)$$

In Eq. (4), L is the pool length, v_{DW} the speed of a dynamic wave, v the average velocity, c the average celerity, while the subindex 0 denotes conditions at the beginning of the transient. A kinematic wave delay $\Delta\tau_{KW}$ is given by

$$\Delta\tau_{KW} = \frac{L}{v_{KW}} = \frac{L}{\frac{1}{B} \frac{dQ}{dy}} \quad (5)$$

where v_{KW} denotes the speed of a kinematic wave, B is the top width, and y the flow depth, while Q and L are as previously defined. Kinematic wave theory assumes a unique relationship between Q and y , that is, a disturbance that travels with no attenuation.

The denominator of Eq. (4) gives the initial speed of a perturbation wave; therefore, $\Delta\tau_{DW}$ estimates the minimum travel time of the flow change. In contrast, v_{KW} is a measure of the ultimate speed attained by the bulk of the wave so that $\Delta\tau_{KW}$ estimates the maximum travel time. Since the concern in determining a delay for use with Eq. (1) is the arrival not of the leading edge nor the bulk of the flow change, but rather of a substantial fraction of that change, a delay value that minimizes water level deviations should be within the range $\Delta\tau_{DW} < \Delta\tau < \Delta\tau_{KW}$.

A delay estimate can be obtained from pool volume changes ΔV and Δq_d

$$\Delta\tau_{\Delta V} = \frac{\Delta V}{\Delta q_d} \quad (6)$$

Eq. (6) was adopted for this study for performance and computational reasons. From a performance standpoint, Bautista et al. (2003) showed that, for the range of flow conditions examined in their study, $\Delta\tau_{\Delta V}$ gives values in the range $\Delta\tau_{DW} < \Delta\tau < \Delta\tau_{KW}$. That study also showed that performance of volume-compensating schedules computed with $\Delta\tau_{\Delta V}$ was only slightly

inferior to the performance of gate-stroking solutions. Computationally, $\Delta\tau_{\Delta V}$ has advantages over Eqs. (4) and (5), first because it can be applied easily to channels of irregular slope and cross section, and second because it matches ΔQ_1 [Eq. (1)] to Δq_d (i.e., $\Delta Q_2=0$). As will be discussed in the following section, volume-compensation calculations are simpler when $\Delta Q_2=0$.

Scheduling of Multiple Demands

Application of Eq. (1) to multiple-pool, multiple-demand problems is straightforward. Starting with the most downstream pool, demands from all offtakes need to be combined and sorted in ascending time order prior to routing in order to enforce the correct sequence of initial conditions. A first upstream check-flow schedule is computed by routing the first-in-time demand change, which is used to update the initial conditions needed to route the second demand.

For example, if $Q(0)$ is the initial inflow of a pool with demand changes Δq_1 and Δq_2 , where $t_{d1} < t_{d2}$, then $Q(0)$ is used to compute ΔV_1 and $\Delta\tau_1$, while $Q(0) + \Delta q_1$ is used to compute ΔV_2 and $\Delta\tau_2$. The subscripts are used here to identify the volume changes and delays associated with each demand change. All remaining demands are routed similarly. Since the upstream schedule of flow changes represents the downstream demand schedule for the next upstream pool, calculations proceed simply by adding these computed demands to the upstream pool's offtake demands. This process is continued, one pool at a time, until reaching the headgate.

The above-described process works best when $\Delta\tau = \Delta V / \Delta q_d$, that is, when $\Delta Q_1 = \Delta q_d$ because each demand change generates one inflow change. In cases where $\Delta Q_1 \neq \Delta q_d$, each offtake demand change generates two inflow changes, each of which will in turn generate two smaller flow changes at the next upstream check. The number of computed flow changes can become very large and their magnitude very small for canals with a large number of pools. Evidently, limiting the number of flow changes would be desirable in practice.

For the case of an arbitrary $\Delta\tau$, Eq. (1) can be recast to route a single change through multiple pools by using cumulative volume change and delay time values. The general expression is given by

$$\Delta Q_{1,m,i} = \frac{\sum_{k=m}^N \Delta V_{k,i}}{N}; \quad t_{1,m,i} = t_{d_i} - \sum_{k=m}^N \Delta\tau_{k,i}$$

$$\Delta Q_{2,m,i} = \Delta q_i - \Delta Q_{1,m,i}; \quad t_{2,m,i} = t_{d_i}$$
(7)

where N =index of pool with demand change; $\Delta Q_{1,m,i}$ =first inflow change for Pool m based on demand change i in Pool N ; $\Delta Q_{2,m,i}$ =second inflow change for Pool m based on demand change i in Pool N ; $t_{1,m,i}$ =time of $\Delta Q_{1,m,i}$; $t_{2,m,i}$ =time of $\Delta Q_{2,m,i}$; $\Delta V_{k,i}$ =volume change needed in Pool k to go from the initial to the final steady state resulting from demand change i in Pool N ; $\Delta\tau_{k,i}$ =time delay for Pool k based on conditions prior to the influence of demand change i in Pool N ; t_{d_i} =time of the demand change i ; and Δq_i =demand change i .

For a given Δq_i , Eq. (7) is applied to every check structure upstream from Pool N . Global check-flow schedules are obtained by superimposing the solutions of individual routing problems.

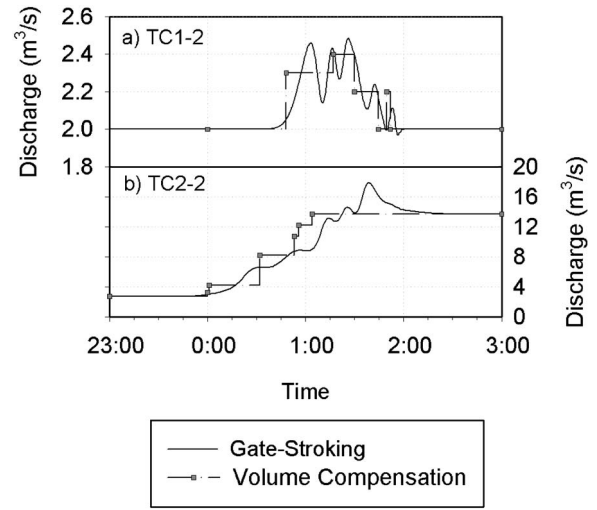


Fig. 7. Headgate gate-stroking and volume-compensating hydrographs: (a) Test Case 1-2 and (b) Test Case 2-2 with volume compensation solutions computed with delay $\Delta\tau_{\Delta V}$

The only difficulty in this process is determining the order in which two or more demand changes need to be routed.

The order depends on the timing of the initial headgate flow adjustment required by each demand change. In other words, the demand change that first affects canal inflow is the change that needs to be routed first, the next change to be routed is the one that affects the canal inflow second, and so on. This order is evident in the simplest of cases, consisting of a single-pool canal with only one offtake, subject to demand changes Δq_1 and Δq_2 where $t_{d1} < t_{d2}$. Clearly, Δq_1 needs to be scheduled first and then used to calculate the new steady-state—i.e., new initial conditions needed to schedule Δq_2 .

Consider next a two-pool canal system subject to two demand changes, Δq_1 in the upstream pool and Δq_2 in the downstream pool, where t_{d1} can be less than, equal to, or greater than t_{d2} . The timing of these initial inflow changes needs to be determined using Eq. (7) and trial and error. A first time estimate $t_{1,1,1}$ is obtained by assuming that the upstream change Δq_1 is the change that needs to be processed first. A second time estimate $t_{1,1,2}$ is obtained next by assuming that the downstream change Δq_2 is the change that needs to be processed first. If $t_{1,1,1} < t_{1,1,2}$, then Δq_1 needs to be routed first, and the schedule for Δq_2 needs to be computed as a function of the new initial conditions produced by Δq_1 . This same approach can be applied to canals with any number of pools and offtakes, with the number of $t_{1,1,i}$ values that need to be computed for each new steady state depending on the number of offtakes. Hence, calculations are carried out one demand change at a time.

Volume-Compensation Routing Example

Volume-compensating feedforward schedules were computed for the two examples presented earlier, TC1-2 and TC2-2, using $\Delta\tau_{\Delta V}$ as the delay. Fig. 7 presents the computed headgate hydrographs along with the corresponding gate-stroking solutions. The effectiveness of both solutions was tested through simulation, using the unsteady-flow program CanalCAD (Holly and Parrish 1995). Tests were carried out, first, assuming ideal flow control at check structures and a tuned feedforward model, that is, check flow was

Table 3. Performance of Volume-Compensation and Gate-Stroking Solutions for Test Case 1-2 with Ideal Flow Control and Tuned Manning n

Performance indicator (%)	Pool 1	Pool 2	Pool 3	Pool 4	Pool 5	Pool 6	Pool 7	Pool 8	Average
Volume compensation									
MAE	4.3	3.9	3.4	2.3	4.8	8.3	6.2	4.2	4.7
IAE	0.3	3.1	0.1	0.5	1.6	0.2	0.1	0.1	0.7
StE	0.0	3.8	0.0	0.7	2.0	0.0	0.0	0.0	0.8
Gate stroking									
MAE	0.4	2.2	3.2	2.3	2.0	3.1	1.9	3.8	2.4
IAE	0.1	1.5	0.2	1.4	1.3	0.2	0.1	0.1	0.6
StE	0.0	2.1	0.0	2.1	2.0	0.1	0.1	0.0	0.8

Note: MAE=maximum absolute error; IAE=integrated average error; and StE=steady-state error.

adjusted at every computational time step to match the requested feedforward changes, and perfect agreement was assumed between unsteady model and either gate-stroking or volume-compensation model parameters.

A second set of simulations was conducted in accordance with some of the guidelines developed by the ASCE Task Committee for testing canal control algorithms (Clemmens et al. 1998). These guidelines restrict the frequency of gate adjustments to maintain the target flow, specify a minimum check gate opening adjustment, and require using different hydraulic parameters (roughness and gate head-discharge relationship) in the control calculations from the ones used in the hydraulic simulation.

The gate-opening constraint and untuned gate relationship were ignored here because they result in inflow-outflow mismatches that cannot be handled by any open-loop control strategy. The flow regulation interval and untuned hydraulic roughness parameters do not affect flow balances, but they affect pool volume and delays. Thus, the impact of both these variables was analyzed. For Test TC1-2, flow adjustments were restricted to once every 5 min, and for TC2-2, once every 15 min. The schedules were adjusted in accordance with this time constraint to deliver the same volume change as the original solution. In addition, the Manning n value used in simulation was increased relative to the value used in feedforward calculations. For Test TC1-2, n was changed from 0.014 to 0.018, while for TC2-2 it was increased from 0.020 to 0.026.

Performance was evaluated using the following expression:

$$\varepsilon_y(t_i) = \frac{\text{abs}(y(t_i) - y_{stp})}{y_{stp}} \times 100; \quad i = 1 \text{ to } T/\Delta T \quad (8)$$

where ε_y =absolute value of relative water depth error; $y(t_i)$ =simulated forebay water depth; y_{stp} =forebay setpoint depth; t_i =discrete time interval; T =total test time (12 h);

and ΔT =sampling interval (5 min). The maximum (maximum absolute error, MAE) and average (integrated absolute error, IAE) values were determined from these time series. An average error was computed also for the last 2 h of the test (steady-state error, StE), a time when the canal should be near steady state. These performance measures also were developed by the ASCE Task Committee on Canal Control Algorithms (Clemmens et al. 1998).

Results

Tables 3 and 4 summarize the performance indicators calculated under ideal flow control and tuned Manning n conditions for each of the two test cases analyzed herein. For TC1-2 (Table 3), average MAE values produced by the volume compensation schedule were double those computed with the gate-stroking schedule. For TC2-2 (Table 4) the difference in average MAE values was fourfold. The average MAE values of Table 3 represent actual deviations of 0.04 and 0.02 m (0.13 and 0.065 ft) for volume compensation and gate stroking, respectively. The corresponding values in Table 4 represent actual deviations of 0.117 and 0.028 m (0.38 and 0.09 ft). Despite the difference in transient deviations, both schedules produced similar (and small) average IAE and StE values. For TC1-2, IAE and StE values represent actual deviations of slightly less than 0.01 m (0.03 ft), while for TC2-2 they represent deviations of less than 0.005 m.

Hence, steady conditions were restored quickly with both schedules and the resulting steady water levels were close to the target in most pools. In a few pools, near-steady conditions were initially attained but water levels later drifted away from their setpoint. This is particularly evident in Pools 2, 4, and 5 in TC1-2 (Table 3), in which StE values exceeded IAE values. These results are explained by small mismatches in pool inflow induced by

Table 4. Performance of Volume-Compensation and Gate-Stroking Solutions for Test Case 2-2 with Ideal Flow Control and Tuned Manning n

Performance indicator (%)	Pool 1	Pool 2	Pool 3	Pool 4	Pool 5	Pool 6	Pool 7	Pool 8	Average
Volume compensation									
MAE	6.3	4.5	4.1	4.6	4.7	6.2	8.1	7.5	5.7
IAE	1.1	0.1	0.1	0.1	0.2	0.3	0.4	0.1	0.3
StE	0.9	0.0	0.0	0.0	0.2	0.2	0.2	0.0	0.2
Gate stroking									
MAE	0.8	1.0	1.9	0.6	0.6	0.6	1.3	5.4	1.5
IAE	0.2	0.2	0.4	0.3	0.1	0.0	0.2	0.6	0.2
StE	0.2	0.1	0.4	0.5	0.1	0.0	0.1	0.3	0.2

Note: MAE=maximum absolute error; IAE=integrated average error; and StE=steady-state error.

Table 5. Performance of Volume-Compensation and Gate-Stroking Solutions for Test Case 1-2 with 5 min Flow Regulation Constraint and Tuned Manning n

Performance indicator (%)	Pool 1	Pool 2	Pool 3	Pool 4	Pool 5	Pool 6	Pool 7	Pool 8	Average
Volume compensation									
MAE	2.9	3.0	4.8	2.7	4.6	3.8	7.4	6.8	4.5
IAE	0.1	0.3	0.1	0.2	0.1	0.1	0.1	0.0	0.1
StE	0.1	0.5	0.0	0.3	0.1	0.0	0.1	0.0	0.1
Gate stroking									
MAE	2.6	3.0	3.7	3.5	2.8	3.4	3.0	4.7	3.3
IAE	0.1	2.0	0.3	2.3	1.3	0.2	0.0	0.1	0.8
StE	0.1	2.7	0.1	3.4	1.3	0.1	0.0	0.0	1.0

Note: MAE=maximum absolute error; IAE=integrated average error; and StE=steady-state error.

Table 6. Performance of Volume-Compensation and Gate-Stroking Solutions for Test Case 2-2 with 15 min Flow Regulation Constraint and Tuned Manning n

Performance indicator (%)	Pool 1	Pool 2	Pool 3	Pool 4	Pool 5	Pool 6	Pool 7	Pool 8	Average
Volume compensation									
MAE	5.6	1.5	2.0	2.7	2.9	2.8	4.9	4.7	3.4
IAE	0.6	0.1	0.2	0.2	0.1	0.3	0.1	0.2	0.2
StE	0.4	0.0	0.2	0.4	0.0	0.2	0.0	0.1	0.2
Gate stroking									
MAE	1.9	1.7	2.0	1.4	1.4	2.7	4.0	4.6	2.5
IAE	0.3	0.1	0.3	0.4	0.2	0.1	0.2	0.3	0.2
StE	0.2	0.0	0.3	0.6	0.2	0.1	0.1	0.2	0.2

Note: MAE=maximum absolute error; IAE=integrated average error; and StE=steady-state error.

Table 7. Performance of Volume-Compensation and Gate-Stroking Solutions for Test Case 1-2 with 5 min Flow Regulation Constraint and Untuned Manning n

Performance indicator (%)	Pool 1	Pool 2	Pool 3	Pool 4	Pool 5	Pool 6	Pool 7	Pool 8	Average
Volume compensation									
MAE	1.3	5.1	6.0	4.0	9.5	10.7	12.5	7.1	7.0
IAE	0.1	3.6	0.2	2.9	1.2	0.6	0.6	0.2	1.2
StE	0.1	4.2	0.1	3.5	1.1	0.1	0.1	0.0	1.1
Gate stroking									
MAE	1.5	8.1	6.2	7.1	12.8	17.4	16.6	9.6	9.9
IAE	0.1	5.3	0.3	5.0	2.4	0.7	0.6	0.2	1.8
StE	0.1	6.5	0.1	6.5	2.2	0.1	0.0	0.0	2.0

Note: MAE=maximum absolute error; IAE=integrated average error; and StE=steady-state error.

Table 8. Performance of Volume-Compensation and Gate-Stroking Solutions for Test Case 2-2 with 15 min Flow Regulation Constraint and Untuned Manning n

Performance indicator (%)	Pool 1	Pool 2	Pool 3	Pool 4	Pool 5	Pool 6	Pool 7	Pool 8	Average
Volume compensation									
MAE	8.1	7.6	3.5	4.5	4.6	5.9	5.5	5.8	5.7
IAE	5.2	4.4	1.6	3.0	3.2	3.0	1.5	0.7	2.8
StE	5.0	3.7	1.1	3.1	3.8	2.7	0.8	0.3	2.6
Gate stroking									
MAE	8.5	7.9	3.3	4.1	4.1	5.8	3.7	4.2	5.2
IAE	5.4	4.5	1.6	2.8	3.0	3.1	1.5	0.9	2.9
StE	5.1	3.7	1.1	3.0	3.6	2.8	0.9	0.3	2.6

Note: MAE=maximum absolute error; IAE=integrated average error; and StE=steady-state error.

numerical accuracy problems, which could not be offset by changes in offtake discharge (the offtakes in those pools closed during the test). Overall results show that volume compensation solutions to multiple-demand problems are effective, although gate-stroking solutions produced better control under the idealized conditions of the test. As expected, the test with largest flow changes, TC2-2, resulted in the largest performance difference.

For both TC1-2 (Table 5) and TC2-2 (Table 6), simulations with the flow regulation constraint resulted in slightly lower performance with the gate-stroking solution when compared to simulations without the constraint (Tables 3 and 4). The flow regulation constraint was expected to negatively affect gate-stroking performance because the method assumes continuous and precise discharge regulation. In contrast, the constraint resulted in slight performance improvements with volume compensation in both tests (Tables 5 and 6 versus Tables 3 and 4).

This improvement may be explained by the fact that the constraint-adjusted volume-compensation schedule varies discharge more gradually than the original solution (the adjusted schedule splits each flow change of the original solution into two flow changes applied over consecutive flow regulation intervals). More gradual discharge variations may help attenuate water-level variations during the early part of the transient. While average IAE and StE values for TC1-2 suggest substantial steady-state performance improvement with the constrained volume-compensation solution (Table 5 versus Table 3), it is important to note again that this test is fairly sensitive to small, numerically induced inflow-outflow mismatches because of the closed offtakes. Thus, the improvement should be considered fortuitous.

As expected, the gate-stroking and volume-compensation schedules did not perform as well under untuned conditions (Tables 7 and 8) in comparison with tuned tests (Tables 5 and 6). Most affected was the gate-stroking solution, as it yielded slightly larger performance indicator values than the volume compensation schedule for TC1-2 (Table 7), while for TC2-2 (Table 8) the resulting indicators were of similar magnitude. The performance loss resulted mainly from volume change errors and inadequate travel time estimates. The volume changes computed with the actual and assumed Manning n value were different by 25% for TC1-2 and almost 60% for TC2-2. Differences in travel time were estimated for TC1-2 from gate-stroking solutions computed at the two values of Manning n considered in the tests, 0.014 and 0.018. The percent increase in travel time was similar to the volume change increase (and thus to the travel time increase computed with $\Delta\tau_{\Delta V}$).

No travel time change estimate was developed for TC2-2 because the gate-stroking algorithm failed to compute a solution at the higher value of Manning n , but results computed at other n values also showed a close correspondence between travel time and volume change variations. Besides volume and timing errors, TC2-2 results also were affected by mismatches between the flows requested by the feedforward schedules and the flows actually delivered during simulation. With the larger Manning n , the simulator predicted smaller head differences across the gates; therefore, flow changes requested by the feedforward solutions could not be supplied at all times during the simulation (the algorithm used to determine gate positions restricted gate openings to 95% of the upstream water depth value, to prevent a computational incident).

It is helpful to examine the observed performance losses in relation to canal properties. In TC1-2, even small-volume errors can produce large water-level deviations because most pools have a relatively short backwater section. However, those volume

errors can be eliminated quickly through increased or decreased offtake discharge. Therefore, despite the large MAE values reported for this test (as large as 17.4% or a 0.14 m [0.46 ft] deviation in Pool 6), IAE and StE values were still small for Pools 1, 3, and 6 through 8, all of which have open offtakes (Table 7).

In contrast, pools in the TC2-2 canal are entirely under backwater. Large-volume change errors translate into moderate water-level deviations, but those errors then can take a long time to correct. This characteristic is reflected in the resulting performance indicators (Table 8). Average MAE values were at most twice those under ideal conditions (Table 4) or with flow control alone (Table 6), but average IAE and StE values were more than 10 times larger than in those tests (or an average error of ± 0.05 m [0.16 ft] by the end of the test).

Discussion

Overall, results suggest that effective feedforward control solutions to multiple-demand problems can be developed with the volume compensation method. However, because of the uncertainty of canal parameters, volume compensation or any other anticipatory control strategy needs to be applied judiciously and preferably implemented in conjunction with a feedback-control strategy.

Central to the volume-compensation method is characterizing pool-volume relationships. Such relationships were easily determined for the hypothetical canals examined here, both of which have regular slope and cross section. Most canals have variable slope and cross section, and in many cases the geometry is known only roughly. Therefore, and especially for geometrically complex channels, extensive simulation and field testing are needed before full implementation to validate the relationships.

In these tests, volume-compensation schedules were computed with $\Delta\tau_{\Delta V}$ as a delay, and the resulting performance was satisfactory under tuned conditions. Similar results were obtained when those schedules were modified to meet the flow regulation interval constraint. In such tests, feedforward changes were applied as much as 2.5 (TC1-2) and 7.5 (TC2-2) min earlier than with the original solution. Therefore, performance does not appear to be critically sensitive to the timing of feedforward changes when canal hydraulic resistance is accurately known.

While no effort was made to assess performance sensitivity to delay estimates under untuned conditions, results do suggest that performance will degrade more as a result of inaccurate volume change estimates than of inaccurate delay estimates. Still, because the delays employed herein are volume-change dependent, the potential for large estimation errors and consequent negative impacts on performance is significant. In fact, initial field experiences with the volume compensation method, conditions under which discharge-volume relationships and hydraulic roughness estimates are both uncertain, have occasionally resulted in clearly mistimed flow changes. Hence, performance of volume-independent delay estimates needs to be examined further under untuned conditions.

Conclusions

Volume-compensation provides a simple, robust, and effective alternative for routing demand changes in open-channel delivery systems. The basic concept, developed for a single-demand

change in a single-pool canal, computes a schedule of inflow variations based on the volume change between the known initial and final desired flow conditions and an estimate of the time needed by the flow change to travel down the canal. The method can be easily extended to multiple-pool, multiple-demand problems by scheduling each demand change separately, subject to its own set of initial conditions, and then superimposing the results. For routine calculations, volume estimates can be derived from tabulated steady-state discharge-volume relationships. Reasonable delay estimates can be generated based on the time needed to supply the required canal volume change.

For the examples presented, which included a case with small-flow changes and one with large-flow changes, performance of volume-compensation solutions was slightly inferior to the performance of solutions obtained with the gate-stroking method, but only with ideal flow control and perfect knowledge of canal hydraulic resistance. There was little difference in performance between methods when applied under constrained and untuned conditions. This is not unexpected because gate-stroking assumes precise knowledge of canal properties (and thus precise knowledge of pool volumes and wave travel times) and unlimited ability to control flows, while the volume-compensation method only requires reasonably accurate knowledge of discharge-volume relations.

Notation

The following symbols are used in this paper:

a, b, c, d = empirical fitting coefficients of discharge-volume relationship;
 B = channel top width;
 c = celerity;
 L = pool length;
 n = Manning roughness coefficient;
 Q = pool discharge;
 q = lateral flow discharge;
 Q_{in} = discharge at pool's upstream boundary;
 Q_n = design discharge;
 Q_{out} = discharge at pool's downstream boundary;
 T = control test total time;
 t_1 = time for first volume-compensation discharge change ΔQ_1 ;
 $t_{1,m,i}$ = time for first volume-compensation discharge change $\Delta Q_{1,m,i}$;
 t_2 = time for second volume-compensation discharge change ΔQ_2 ;
 $t_{2,m,i}$ = time for second volume-compensation discharge change $\Delta Q_{2,m,i}$;
 t_d = demand change time;
 t_i = discrete time value;
 V = pool volume;
 v = average flow velocity;
 v_{DW} = speed of dynamic wave;
 v_{KW} = speed of kinematic wave;
 y = water depth at pool's forebay;
 y_{stp} = pool forebay setpoint depth;
 ΔQ_1 = first volume-compensation pool inflow rate change;

$\Delta Q_{1,m,i}$ = first volume-compensation pool inflow rate change for Pool m based on demand change i in Pool N ;
 ΔQ_2 = second volume-compensation pool inflow rate change;
 $\Delta Q_{2,m,i}$ = second volume-compensation pool inflow rate change for Pool m based on demand change i in Pool N ;
 Δq_d = demand change;
 ΔT = water depth sampling interval;
 ΔV = difference in pool volume between initial and final steady states;
 $\Delta \tau$ = delay;
 $\Delta \tau_{DW}$ = dynamic wave delay;
 $\Delta \tau_{KW}$ = kinematic wave delay;
 $\Delta \tau_{\Delta V}$ = volume change-based delay; and
 ε_y = absolute value of relative water-level error.

References

- Bautista, E., and Clemmens, A. J. (1999a). "Computerized anticipatory control of irrigation delivery systems." *Proc., USCID Workshop on Modernization of Irrigation Water Delivery Systems*, 359–373.
- Bautista, E., and Clemmens, A. J. (1999b). "Response to the ASCE Task Committee test cases to open-loop control measures." *J. Irrig. Drain. Eng.*, 125(4), 179–188.
- Bautista, E., Clemmens, A. J., and Strelkoff, T. S. (1997). "Comparison of numerical procedures for gate stroking." *J. Irrig. Drain. Eng.*, 123(2), 129–136.
- Bautista, E., Clemmens, A. J., and Strelkoff, T. S. (2002). "Routing demand changes with volume compensation: An update." *Proc., USCID/EWRI Conf.*, 367–376.
- Bautista, E., Strelkoff, T. S., and Clemmens, A. J. (2003). "General characteristics of solutions to the open-channel flow, feedforward control problem." *J. Irrig. Drain. Eng.*, 129(2), 129–137.
- Clemmens, A. J., Kacerek, T. F., Grawitz, B., and Schuurmans, W. (1998). "Test cases for canal control algorithms." *J. Irrig. Drain. Eng.*, 124(1), 23–30.
- Corriga, G., Fanni, A., Sanna, S., and Usai, G. (1982). "A constant-volume control method for open channel operation." *Int. J. Model. Simulat.*, 2(2), 108–112.
- Cunge, J. A., Holly, F. M., and Verwey, A. (1980). *Practical aspects of computational river hydraulics*, Pitman, Boston.
- Deltour, J. L. (1992). "Application de l'automatique numerique a la regulation des canaux." Doctoral thesis, Institute Mecanique de Grenoble, Grenoble, France.
- Falvey, H. T., and Luning, P. C. (1979). "Gate stroking." *Rep. REC-ERC-79-7*, United States Bureau of Reclamation, United States Department of the Interior, Washington, D.C.
- Henderson, F. M. (1966). *Open-channel flow*, MacMillan, New York.
- Holly, F. M., Jr., and Parrish, J. B. (1995). *CanalCAD: Dynamic flow simulation in irrigation canals with automatic gate control*, Iowa Institute of Hydraulic Research, Iowa City, Iowa.
- Papageorgiou, M., and Messmer, A. (1985). "Continuous-time and discrete-time design of water flow and water level regulators." *Automatica*, 21(6), 649–661.
- Parrish, J. B. (1997). "Idealized automated control of sloping canals." *J. Irrig. Drain. Eng.*, 123(4), 270–278.
- Strelkoff, T. S., and Clemmens, A. J. (1998). "Nondimensional expression of unsteady canal flow." *J. Irrig. Drain. Eng.*, 124(1), 59–62.
- Wylie, E. B. (1969). "Control of transient free surface flow." *J. Hydraul. Div., Am. Soc. Civ. Eng.*, 95(1), 347–361.